Infrared Spectra and Density Functional Theory Calculations of Group 10 Transition Metal Sulfide Molecules and Complexes

Binyong Liang, Xuefeng Wang, and Lester Andrews*

Department of Chemistry, University of Virginia, P.O. Box 400319, Charlottesville, Virginia 22904-4319

Received: December 8, 2008; Revised Manuscript Received: January 22, 2009

Laser-ablated Ni, Pd, and Pt atoms were reacted with sulfur molecules emerging from a microwave discharge in argon during condensation at 7 K. Reaction products were identified from matrix infrared spectra, sulfur isotopic shifts, spectra of sulfur isotopic mixtures, and frequencies from density functional calculations. The strongest absorptions are observed at 597.9, 596.1, and 583.6 cm^{-1}, respectively, for the group 10 metals. These absorptions show large sulfur-34 shifts and 32/34 isotopic frequency ratios (1.0282, 1.0285, 1.0298) that are appropriate for S−S stretching modes. Of most importance, mixed 32/34 isotopic 1/4/4/2/4/1 sextets identify this product with two equivalent S_2 molecules containing equivalent atomic positions as the bisdisulfur π complexes $M(S_2)_2$. Our DFT calculations find stable D_{2h} structures with B_{1u} ground states and intense b_{1u} infrared active modes a few wavenumbers higher than the observed values. A minor Ni product at 505.8, 502.7 cm^{-1} shows the proper sulfur-34 shift for assignment to ^{58}NiS, ^{60}NiS. Another major product with Pt at 512.2 cm^{-1} reveals an asymmetric triplet absorption with mixed sulfur 32/34, which is appropriate for assignment to the SPtS disulfide molecule. A weak 491.7 cm^{-1} peak exhibits the sulfur-34 shift expected for PtS, and this assignment follows.

Introduction

Transition metal sulfides find numerous applications as biochemical and industrial catalysts.[1] The removal of sulfur from crude oil is a major catalytic process, and Ni-based anodes degrade from sulfur in fuels. DFT calculations of electronic and vibrational properties of several nickel sulfides observed on Ni-based anodes in solid oxide fuel cells have been performed.[2] Such solid nickel sulfides present several stoichiometries. In addition, nickel-based anodes degrade from sulfur content in fuels.[3] Interestingly, NiS forms nanowhiskers in hydrothermal reactions.[4] The more noble metals Pd and Pt are less reactive with sulfur. The correlation between electronic properties and the hydro-desulfurization activity of 4d transition metal sulfides including PdS and PdS_2 and the electrochemical reduction of H_2S on Pt have been investigated.[5,6] In addition, PdS and PtS nanoparticles have been synthesized.[7]

A major chemical interest is in comparison of metal oxides and sulfides. Reactions of thermal Ni, Pd, and Pt atoms with O_2 were investigated by the Ozin group, and side-bound dioxygen complexes $M(O_2)_{1,2}$ were identified.[8,9] Later reactions with laser-ablated metal atoms provided sufficient excess energy to form in addition the NiO, NiO_2, PtO, and PtO_2 oxide molecules.[10−12] Previous reactions of groups 4 and 5 transition metals and the early actinides Th and U with small sulfur molecules gave mostly monosulfide and disulfide molecular products.[13−16] Thus, we anticipate that metal sulfides will also be produced here. Reports of group 10 sulfide molecules are limited to a Ni and OCS reaction product in solid argon and rotational spectroscopy of NiS and PtS.[17−20] Two important theoretical investigations of the first row transition metal sulfides[21,22] are relevant to our observation of NiS in the matrix infrared spectrum.

The present work reports the reaction of laser-ablated Ni, Pd, and Pt atoms with small sulfur molecules $S_{2,3,4}$ produced through microwave discharge of elemental sulfur vapor[23] and density functional calculations of the anticipated product molecules. Since our earlier work on infrared spectra of S_3 and S_4 in solid argon using sulfur-34 substitution to help characterize these molecules,[23] their microwave spectra and high level electronic structure calculations have been reported.[24−26]

Experimental and Computational Methods

A microwave discharge in argon seeded with sulfur vapor was used as a source of sulfur atoms and small molecules as reagents for group 10 transition metal atoms. The coaxial quartz discharge tube evolved from that used in earlier experiments.[23] Natural isotopic sulfur (Electronic Space Products, Inc., recrystallized) and enriched sulfur (98% ^{34}S, Cambridge Isotope Laboratories) were used as received; different mixtures of the two isotopic samples were also employed. The vapor pressure of sulfur feeding the discharge was controlled by resistance heating. The microwave discharge was maintained in the argon−sulfur mixture by an Opthos Instruments 120 W microwave discharge (using 30−50% of the maximum power level) with an Evenson−Broida cavity and extended from 5 cm downstream of the sulfur reservoir to the end of the discharge tube. The presence of S_2 in the discharge was determined by appearance of the characteristic blue emission.[27]

The experimental method for laser ablation and matrix isolation has been described in detail previously.[28−30] Briefly, the Nd:YAG laser fundamental (1064 nm, 10 Hz repetition rate with 10 ns pulse width, 3−5 mJ/pulse) was focused to ablate rotating Ni and Pd (Johnson−Matthey) or Pt (crucible piece, American Platinum Works) metal targets. Laser-ablated metal atoms were codeposited with a sulfur-doped argon stream onto a 7 K CsI cryogenic window at 2−4 mmol/h for 0.5−1.5 h. Infrared spectra were recorded at 0.5 cm^{-1} resolution on a

---

* Corresponding author. E-mail: lsa@virginia.edu.

10.1021/jp810795q CCC: $40.75

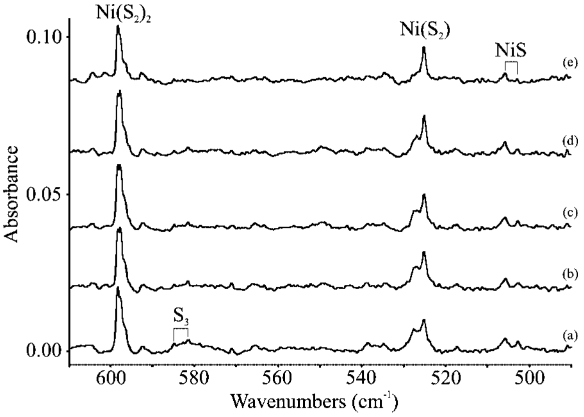

Figure 1. Infrared spectra in the 620−480 cm^{-1} region for products formed in the laser-ablated Ni reaction with discharged sulfur vapor during condensation in excess argon at 7 K. (a) Sample deposited for 60 min, (b) after annealing to 30 K, (c) after >220 nm irradiation, (d) after annealing to 35 K, and (e) after annealing to 43 K.

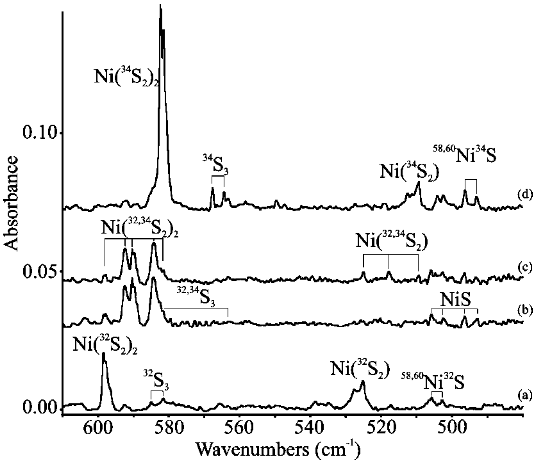

Figure 2. Infrared spectra in the 610−480 cm^{-1} region for products formed in the laser-ablated Ni reaction with discharged sulfur-34 enriched vapor during condensation in excess argon at 7 K. (a) Normal ^{32}S isotopic sample deposited for 60 min, (b) 50/50 mixed ^{32,34}S isotopic sample, (c) after annealing to 40 K, and (d) ^{34}S after sample deposition.

Nicolet 550 spectrometer with 0.1 cm^{-1} accuracy using a mercury cadmium telluride detector. Matrix samples were annealed at different temperatures, and selected samples were subjected to irradiation using a medium-pressure mercury lamp (>220 nm) with the globe removed.

Following previous work,[13,14,30] DFT calculations were performed on anticipated metal sulfide products first using the Gaussian 98 program,[31] the B3LYP density functional,[32] the 6-311+G(d) basis set for sulfur and nickel, and the LanL2DZ effective core potential and basis for Pd and Pt.[33,34] Additional calculations were performed using the Gaussian 03 program system,[35] the B3LYP density functional,[32] and the large Gaussian basis 6-311+G(3df) for S and SDD pseudopotential and basis for the metal atoms.[33,36]

Results and Discussion

Infrared Spectra. The microwave discharge of elemental sulfur vapor in a flowing argon stream gives S_2 as judged from its blue emission[27] and S_3 and S_4 based on their known infrared absorption spectra.[23] Laser-ablated precious metal atoms were codeposited with such an argon stream containing sulfur species, and new metal-dependent reaction product spectra will be presented and assigned. Relatively low laser energy was employed such that the concentration of metal atoms is sufficiently low as to minimize the contribution of dimetal species to the observed spectra.

Ni + S$_x$. Seven experiments were done with nickel and sulfur vapor varying the sulfur content by a factor of 5 as judged by the strong S_3 absorption intensities and the ablation laser energy over a 10-fold range. These are very difficult matrix isolation experiments to perform as there are a large number of variables to control. A representative set of spectra for a medium reagent concentration is illustrated in Figure 1, where the strong S_3 absorptions in the 600 cm^{-1} region (not shown) are twice as strong as the S_4 absorptions. The major peak is probably split by the matrix at 598.5 and 597.9 cm^{-1} and is little changed on annealing to 30 K or full mercury arc irradiation, but decreases on annealing to higher temperatures. Two weak bands at 584.9 and 581.7 cm^{-1} arise from the symmetric stretching mode of the bent S_3 molecule in two different argon matrix sites.[23] The 525.2 cm^{-1} band sharpens and increases slightly on annealing. A weak 505.8, 502.7 cm^{-1} doublet also sharpens on early annealing and decreases on late annealing.

These bands exhibit substantial sulfur-34 isotopic shifts as revealed in Figure 2d and Table 1. The mixed sulfur-32, 34 isotopic spectra show important diagnostic multiplets (Figure 2b,c): the strongest feature contains three new intermediate mixed isotopic bands at 592.5, 590.4, 584.4 cm^{-1}. The 525.2 cm^{-1} band that increases on annealing also reveals one intermediate isotopic component at 517.8 cm^{-1}. The weak doublet at 505.8, 502.7 cm^{-1} with 2/1 relative intensity forms a matching 2/1 doublet with its sulfur-34 counterpart at 496.3, 493.2 cm^{-1}.

Pd + S$_x$. The palladium reaction with sulfur molecules gave a new matrix-split doublet at 597.4, 596.1 cm^{-1} and bands at 549.4, 524.3, and 495.5 cm^{-1}. Annealing decreased the 597.4 cm^{-1} component in favor of the 596.1 cm^{-1} peak, and the 524.3 cm^{-1} band increased while the 524.3 and 495.5 cm^{-1} bands decreased (Figure 3). A weak new absorption at 580.0 cm^{-1} increased slightly on annealing. Full arc photolysis again had little effect on the spectrum. Similar shifted bands were observed with sulfur-34, and the frequencies are listed in Table 1. The removal of the upper matrix site on the major band is particularly advantageous with the 50/50 mixed 32, 34 isotopic spectrum, which reveals a 1/4/4/2/4/1 relative intensity sextet. Higher multiplets were also observed for the three lower bands.

Pt + S$_x$. The platinum reaction products gave the sharpest product absorptions as illustrated in Figure 4. As before, annealing and UV irradiation had little effect on the upper band, now at 583.6 cm^{-1}, but another band at 512.2 cm^{-1} decreased slightly on this treatment. A weak 534.2 cm^{-1} band increased on annealing but decreased on UV photolysis, whereas a weak 491.7 cm^{-1} band sharpened. These absorptions exhibited sulfur-34 isotopic frequency shifts and different 32/34 isotopic frequency ratios (Figure 5 and Table 1), which reveal the relative participations of Pt and S in the normal vibrational modes. Of equal importance, the isotopic multiplets using mixed sulfur 32, 34 produced intermediate components that provide stoichiometric information. The sharp 583.6 cm^{-1} band gave rise to a 1/4/4/2/4/1 relative intensity sextet, the 534.2 cm^{-1} band showed two weak mixed isotopic components, the 512.2 cm^{-1} feature led to an asymmetric triplet with a possible weak additional band at 484.2 cm^{-1}, and the 491.7 cm^{-1} band revealed only pure isotopic counterparts.

Calculations. Although sulfur molecules are very difficult to model with electronic structure calculations,[25,26] our B3LYP result for thiozone (Table 2) is in very good agreement with

TABLE 1: Infrared Absorptions from Codeposition of Laser-Ablated Ni, Pd, and Pt Atoms with Discharged Sulfur Vapor in Excess Argon

^{32}S	^{34}S	$^{32}S + ^{34}S$	$R(32/34)$	identity
		Nickel		
598.5	582.3	598.4, 592.5, 590.4, 584.4, 582.3	1.0278	$Ni(S_2)_2$
597.9	581.5	597.8, 592.5, 589.7, 584.4, 581.5	1.0282	$Ni(S_2)_2$ site
584.9	567.7		1.0303	S_3, ν_1
581.7	564.4		1.0307	S_3, ν_1
525.2	509.4	525.2, 517.8, 509.4	1.0310	$Ni(S_2)$
505.8	496.3	505.8, 496.3	1.01914	^{58}NiS
502.7	493.2	502.7, 493.2	1.01926	^{60}NiS
		Palladium		
597.4	580.5	597.4, 592.5 589.0, 586.6, 584.1, 580.5	1.0291	$Pd(S_2)_2$ site
596.1	579.6	596.1, 591.4, 587.9, 585.8, 583.3, 579.6	1.0285	$Pd(S_2)_2$
591.4	574.9		1.0287	$Pd(S_2)$
584.9	567.7		1.0303	S_3, ν_1
581.7	564.4		1.0307	S_3, ν_1
549.4	533.5	544.7, 541.5, 539.5, 537.5	1.0298	$Pd(S_x)$
524.3	508.9	524.3, 521.0, 519.6, 517.2, 512.8, 509.1	1.0303	$Pd(S_x)$
495.5	481.6	491.9, 488.3, 485.0	1.0289	$Pd(S_x)$
		Platinum		
583.6	566.7	583.6, 578.5, 575.2, 571.8, 570.0, 566.7	1.0298	$Pt(S_2)_2$
534.2	518.4	534.2, 531.4, 523.6, 518.4	1.0305	$Pt(S_2)$
512.2	500.6	512.2, 508.1, 500.6	1.0232	PtS_2
509.2	497.6	509.2, 505.1, 497.6	1.0233	PtS_2 site
491.7	479.3	491.7, 479.3	1.0259	PtS
488.9	476.8	488.9, 476.8	1.0254	PtS site

experiment.[23,24] Following computations on the analogous oxide systems, the side-bound $Ni(S_2)$ structure is the global minimum energy species in the $^3B_1$ state, the side-bound $^1A_1$ species is 26 kcal/mol higher, and the open $^1A_1$ SNiS state is 30 kcal/mol higher in energy, in contrast to the corresponding nickel oxide species.[10] Calculations with the larger Gaussian basis set on S and SDD on Ni gave almost the same structures and slightly higher frequencies. Computed parameters are listed in Table 2. The global minimum energy $Ni(S_3)$ species is the C_{2v} four-membered ring in the $^3A_2$ state. The $^3B_1$ (+9 kcal/mol) and $^3B_2$ (+38 kcal/mol) states are higher in energy. The nickel bisdisulfur species has an imaginary frequency in the D_{2d} structure, but stable D_{2h} structures were found with the $^3B_{1u}$ 13 kcal/mol lower than the ^1A_g state. The NiS molecule is computed to have the $^3\Sigma^-$ ground state, in agreement with previous workers,[21,22] and 1.986 Å bond length and 512.2 cm^{-1} harmonic frequency with the small basis and 1.966 Å and 513.2 cm^{-1} with the large basis.

The ground-state $Pd(S_2)$, $Pd(S_2)_2$, and $Pt(S_2)_2$ symmetries are the same as found for the Ni species, but $^3B_1$ $Pt(S_2)$ has an imaginary frequency, and the cyclic $^1A_1$ state converges to the lower energy $^1\Sigma_g^+$ linear disulfide SPtS molecule analogous to OPtO.[11,12] In contrast, the $Pd(O_2)$ and $Pt(O_2)$ ground states were found to be $^1A_1$.[12] Although the ground state of PtS is XO^+ for Hund's case (c), our DFT calculation for singlet and triplet Σ states gives 500 cm^{-1} for the harmonic frequency, which is near the 511(5) cm^{-1} value deduced from the microwave spectrum.[20]

Stable $Pd(O_2)_2$ and $Pt(O_2)_2$ structures were computed for ^1A_g states in D_{2h} symmetry, which provided a reasonable fit to the experimental frequencies.[12] We have repeated these calculations and find similar structures for $^3B_{1u}$ states that are 29, 33, and 31 kcal/mol lower in energy than the corresponding ^1A_g states. The bisdioxygen and disulfur species are π complexes according to NBO analysis.[35,37] Table 3 lists the Mulliken charges, spin densities, and complex bonding orbital compositions. Table 4

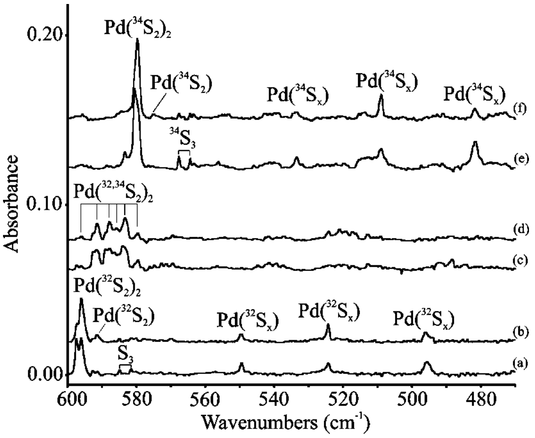

Figure 3. Infrared spectra in the 600−470 cm^{-1} region for products formed in the laser-ablated Pd reaction with discharged sulfur vapor during condensation in excess argon at 7 K. (a) Normal ^{32}S sample deposited for 60 min, (b) after annealing to 40 K, (c) 50/50 $^{32}S/^{34}S$ sample deposited, (d) after annealing to 40 K, (e) ^{34}S after sample deposition, and (f) after annealing to 40 K.

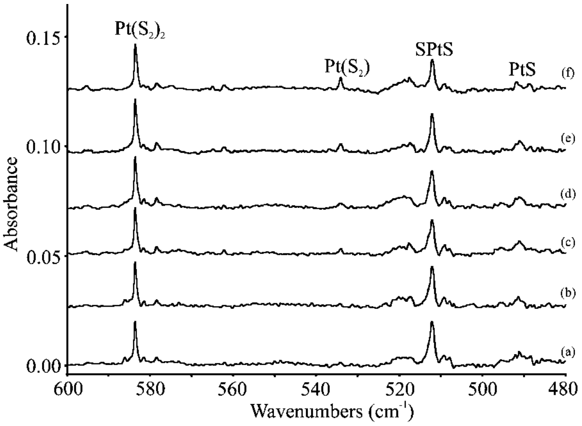

Figure 4. Infrared spectra in the 600−480 cm^{-1} region for products formed in the laser-ablated Pt reaction with discharged sulfur vapor during condensation in excess argon at 7 K. (a) Sample deposited for 60 min, (b) after annealing to 25 K, (c) after annealing to 30 K, (d) after >220 nm irradiation, (e) after annealing to 35 K, and (f) after annealing to 40 K.

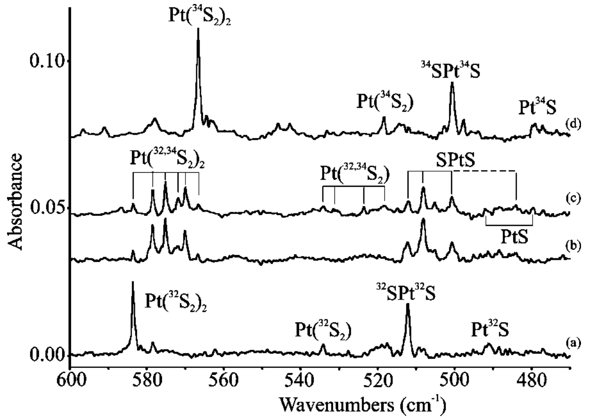

Figure 5. Infrared spectra in the 600−470 cm^{-1} region for products formed in the laser-ablated Pt reaction with discharged sulfur-34 enriched vapor during condensation in excess argon at 7 K. (a) Normal ^{32}S sample deposited for 60 min and after annealing to 35 K, (b) 50/50 mixed $^{32,34}S$ isotopic sample after deposition, (c) after annealing to 43 K, and (d) ^{34}S sample after deposition and annealing to 35 K.

gives the structural parameters and frequencies calculated for the bisdioxygen complexes for comparison with those for the bisdisulfur complexes.

Figure 6 illustrates structures calculated for the important group 10 metal sulfur species, which were observed in these experiments, except for PdS.

NiS. The 505.8, 502.7 cm^{-1} doublet has the appropriate relative intensities (2/1), position, and separation to be due to the ground-state NiS molecule with the dominant natural nickel 58 and 60 natural isiotopes.[38] Our DFT calculation predicted 513.2, 510.1 cm^{-1} for the ^{58}NiS and ^{60}NiS harmonic frequencies, the same isotopic separation as observed within experimental accuracy. Furthermore, our DFT calculation also found a 9.8 cm^{-1} sulfur-34 shift in harmonic frequencies, and we observed a 9.5 cm^{-1} shift (32/34 isotopic frequency ratio 1.0191): this difference is appropriate for the slight difference in anharmonicity for motions of the two different sulfur isotopes against the nickel mass. Another DFT calculation also predicted 513 cm^{-1}, and the rotational constant and dissociation energy gave 507 cm^{-1} for the harmonic frequency.[18,22] Even though the NiS ground state is a multireference problem,[21] DFT predicts the fundamental frequency accurately. In addition, the gas-phase near IR spectrum currently under analysis reveals a 505.0 cm^{-1} fundamental frequency.[39] Hence, the recent results are in agreement for the NiS molecule vibrational fundamental.

$Ni(S_2)$. The 525.2 cm^{-1} band increases slightly on annealing and shifts to 509.4 cm^{-1} with sulfur-34 (32/34 isotopic frequency ratio 1.0310). It exhibits a single intermediate mixed isotopic component at 517.8 cm^{-1}. This is a pure sulfur vibrational mode, and it suggests an intact S_2 molecule bound to Ni in a spontaneous reaction of reagent materials. Because $Ni(S_2)$ is the global minimum energy for this stoichiometry (Table 2), and the strongest calculated mode is the symmetric S−S stretching mode at 534 cm^{-1}, in excellent agreement with observation, the 525.2 cm^{-1} band is assigned to $Ni(S_2)$. Considering that the infrared intensitiy for the strongest $Ni(S_2)$ mode is 10% of that for the larger $Ni(S_2)_2$ complex, the spectra reveal a larger yield of the primary $Ni(S_2)$ complex.

$Ni(S_2)_2$. The strongest absorption at 598.5 cm^{-1} shifts to 582.3 cm^{-1} with sulfur-34 (32/34 frequency ratio 1.0278), which is almost up to that for a pure S−S stretching mode (the S_3 stretching modes average 1.0305),[23] but slight coupling with Ni motion is evidenced from the computed 0.6 cm^{-1} Ni 58−60 isotopic shift. The important diagnostic information here is the observation of three strong intermediate mixed isotopic bands (Figure 2), which is similar to the mixed oxygen isotopic spectrum observed for $Ni(O_2)_2$.[8,10] Our calculation for ground-state $Ni(S_2)_2$ predicts the strongest b_{1u} fundamental at 602.9 cm^{-1} and the three strongest mixed isotopic bands for (32−32)Ni(32−34), (32−34)Ni(32−34), and (32−34)Ni(34−34) to be red-shifted 6.7, 8.0, and 15.0 cm^{-1}, respectively, from the 598.5 cm^{-1} normal isotopic band, and the observed bands are shifted by 6.0, 8.1, and 14.1 cm^{-1}. The weaker mixed isotopic peak for (32−32)Ni(34−34) is too close to the latter to be resolved. The isotopic shifts and mixed isotopic pattern and the agreement in band position and isotopic pattern with our DFT calculation confirm this observation and assignment to $Ni(S_2)_2$.

$Pd(S_2)_2$. The major Pd product at 596.1 cm^{-1} shifts to 579.6 cm^{-1} with sulfur-34 (1.0291 isotopic frequency ratio) and forms a 1/4/4/2/4/1 relative intensity sextet with mixed sulfur-32, 34, which reveals the presence of two equivalent S_2 subunits with equivalent S atomic positions, just as found for $Pd(O_2)_2$.[9] Our DFT calculation predicted the harmonic frequency as 604 cm^{-1} and mixed isotopic splittings within the range of 0.0−1.1 cm^{-1} agreement with the observed values. The observed isotopic multiplet and shifts substantiate the observation of the $Pd(S_2)_2$ complex in these experiments.

$Pd(S_2)$. The $Pd(S_2)$ complex is predicted to have a very weak absorption near 584 cm^{-1}, and this region contains weak bands for the S_3 reagent and a weak new absorption at 591.4 cm^{-1} just below $Pd(S_2)_2$ that is not present with Ni and Pt. This band appears at 574.9 cm^{-1} with sulfur-34, and the ratio (1.0287) is appropriate for the S−S stretching mode in the $Pd(S_2)$ complex. These bands increase slightly on annealing and photolysis as is expected for this primary complex, which is a first step in the straightforward formation of the bis $Pd(S_2)_2$ complex.

$Pd(S_x)$. The three weak bands at 549.4, 524.3, 495.5 cm^{-1} with Pd all show mixed isotopic multiplets that require $x = 3$ or 4, but we cannot identify these molecules with certainty. Our calculation for $Pd(S_3)$ predicts a strong b_2 mode at 505 cm^{-1} (Table 2), and this is reasonable for the 495.5 cm^{-1} band or even the 524.3 cm^{-1} absorption. Different structural isomers are possible, and these heavy metal sulfur species are difficult to model computationally.

PdS. The PdS molecule is computed to absorb very weakly at 426 cm^{-1}, which is too low and too weak to be observed here. The lack of observation of the more favorable PdO molecule[12] makes the formation and observation of PdS problematic.

$Pt(S_2)_2$. The sharp, stable platinum product absorption at 583.6 cm^{-1} also becomes a 1/4/4/2/4/1 relative intensity sextet with mixed sulfur-32, 34, which again demonstrates the presence of two equivalent S_2 subunits with equivalent S atomic positions, just as found for $Pt(O_2)_2$.[9,11,12] Our DFT calculation predicted the strongest infrared absorption, the antisymmetric b_{1u} S−S stretching mode, at 595.8 cm^{-1}, and this mode at 590.4 cm^{-1} for the four (32−32)Pt(32−34) isotopic molecules, at 587.0 cm^{-1} for the four (32−34)Pt(32−34) possibilities, at 583.4 cm^{-1} for the two (32−32)Pt(34−34) modifications, at 581.5 cm^{-1} for the four (32−34)Pt(34−34) isotopic species, and at 578.1 cm^{-1} for the all-34 substitution. Thus, the five spacings within the sextet are calculated [observed] as 5.4 [5.1], 3.4 [3.3], 3.6 [3.4], 1.9 [1.8], and 3.4 [3.3] cm^{-1}. This excellent agreement is well within the accuracy of both computational and experimental determinations, and it certainly substantiates our assignment to the platinum bisdisulfur molecule in the ground $^3B_{1u}$ state as calculated.

TABLE 2: Calculated Structural Parameters and Vibrational Frequencies (cm^{-1}) for Group 10 Sulfide Molecules and Complexes[a]

species	state	lengths, Å; angles, deg	rel. ener. (kcal/mol)	frequencies, cm^{-1} (symmetry, intensities, km/mol)
S_2	$^3\Sigma_g^-$	SS: 1.902	0	715.9 (0)
S_3	$^1A_1$	SS: 1.922 SSS: 118.5	0	686.5 (b_2,134), 594.5 (a_1,2), 262.3 (a_1,1)
NiS	$^3\Sigma^-$	NiS: 1.966	0	Ni^{32}S: 513.2(21); Ni^{34}S: 503.4(20)
Ni(S_2)	$^3B_1$	NiS: 2.155 SS: 2.070	0	528.0 (a_1,6), 290.2 (a_1,2), 243.0 (b_2,2)
SNiS	$^1A_1$	NiS: 1.938 SNiS: 130.2	30	596.0 (b_2,32), 485.1 (a_1,6), 55.7 (a_1,2)
Ni(S_3) (C_{2v})	$^3A_2$	NiS: 2.266 SS: 2.028 SSS: 104.1	0	514 (a_1,0), 510 (b_2,87), 313 (a_1,1), 225 (a_1,7), 220 (b_2,7), 61 (b_1,4)
Ni(S_2)$_2$ (D_{2h})	$^3B_{1u}$	NiS: 2.168 SS: 1.989 SNiS: 125.4	0	611 (a_g,0), 603 (b_{1u},60), 385 (b_{1u},2), 301 (b_{2u},1), 274 ($b_{3\,g}$,0), 253 (a_g,0), 118 (a_u,0), 113 (b_{3u},0), 104 (b_{2u},0)
Ni(S_4)	^3B	NiS: 2.183 SS: 2.021, 2.157	19	494 (b,54), 487 (a,0), 402 (a,4), 312 (a,1), 300 (b,22), 225 (b,23), 158 (a,4), 96 (a,0), 88 (b,5)
Ni(S_4) (C_{2v})	$^3B_2$	NiS: 2.183 SS: 2.021, 2.157	21	515 (a_1,3), 502 (b_2,81), 357 (a_1,4), 356 (b_2,4), 317 (a_1,0), 247 (b_2,0), 153 (a_1,6), 105 (b_1,2), 11i (a_2,0)
PdS	$^3\Sigma^-$	PdS: 2.126	0	Pd^{32}S: 425.9(1); Pd^{34}S: 416.2(1)
Pd(S_2)	$^3B_1$	PdS: 2.362 SS: 2.021	0	584 (a_1,4), 249 (a_1,0), 143 (b_2,0)
Pd(S_2)	$^1A_1$	PdS: 2.319 SS: 2.021	4	580 (a_1,0), 303 (a_1,0), 239 (b_2,1)
SPdS	$^3A_2$	PdS: 2.123 SSS: 115.2	32	434 (b_2,16), 427 (a_1,1), 115 (a_1,1)
Pd(S_3) (C_{2v})	$^3A_2$	PdS: 2.397 SS: 2.023 SSS: 101.6	0	530 (a_1,0), 505 (b_2,51), 296 (a_1,2), 207 (a_1,1), 200 (b_2,7), 75 (b_1,2)
Pd(S_2)$_2$ (D_{2h})	$^3B_{1u}$	PdS: 2.350 SS: 1.976 SPdS: 130.3	0	625 (a_g,0), 604 (b_{1u},83), 318 (b_{1u},6), 248 ($b_{3\,g}$,0), 248 (a_g,0), 238 (b_{2u},0), 117 (a_u,0), 94 (b_{2u},1), 92 (b_{3u},0)
PtS	$^3\Sigma$, $^1\Sigma$	PtS: 2.07	0	Pt^{32}S: 500.6(2); Pt^{34}S: 487.8(2)
SPtS	$^1\Sigma_g^+$	PtS: 2.086	0	Pt^{32}S$_2$: 525.9 (σ_u,56), 508.7 (σ_g,0), 30.0 (π_u,0 × 2) ^{32}SPt^{34}S: 522.1 (σ,50), 499.0 (σ,5), 29.7 (π,0 × 2) Pt^{34}S$_2$: 514.1 (σ_u,53), 493.5 (σ_g,0), 29.3 (π_u,0 × 2)
Pt(S_2)	$^3B_1$	PdS: 2.302 SS: 2.057	8	535 (a_1,2), 257 (a_1,0), 13 (b_2,6)
Pt(S_3) (C_{2v})	$^3A_2$	PtS: 2.345 SS: 2.038 SSS: 98.4	0	513 (a_1,0), 478 (b_2,42), 337 (a_1,1), 213 (a_1,1), 189 (b_2,o), 46 (b_1,1)
Pt(S_2)$_2$ (D_{2h})	$^3B_{1u}$	PtS: 2.346 SS: 1.989 SPtS: 129.8	0	616 (a_g,0), 595.8 (b_{1u},54), 290 (b_{1u},2), 282 (a_g,0), 270 ($b_{3\,g}$,0), 182 (b_{2u},3), 115 (a_u,0), 103 (b_{2u},0), 95 (b_{3u},0) [590.4, 587.0, 583.4, 581.5, 578.1 (b_{1u}) for $^{34}S_{1,2,2,3,4}$]

[a] Calculations used B3LYP/6-311+G(3df)/SDD.

TABLE 3: Mulliken Charges and Spin Densities Calculated for the $^3B_{1u}$ Ground States of D_{2h} Structured Group 10 Metal Bisdioxide and Bisdisulfide π Complexes and the $^3B_1$ Ground States of the C_{2v} Disulfide π Complexes[a]

	qM	qO/S	spin M, O/S	M—O/S bonding[b]
Ni(O_2)$_2$	+0.92	−0.23	0.00, 0.50	(0.98) 87% O (94% p, 6% s)−13% Ni (47% s, 52% d)
Pd(O_2)$_2$	+0.69	−0.17	0.00, 0.50	(0.96) 85% O (96% p, 3% s)−15% Ni (46% s, 53% d)
Pt(O_2)$_2$	+0.93	−0.23	0.08, 0.48	(0.98) 81% O (93% p, 6% s)−19% Ni (42% s, 58% d)
Ni(S_2)$_2$	+0.028	−0.007	0.20, 0.45	(0.96) 76% S (92% p, 8%s)−24% Ni (48% s, 51% d)
Pd(S_2)$_2$	+1.33	−0.33	0.030, 0.493	(0.95) 75% S (94% p, 6% s)−25% Ni (48% s, 51% d)
Pt(S_2)$_2$	+0.98	−0.245	0.104, 0.474	(0.97) 70% S (92% p, 7% s)−30% Ni (46% s, 53% d)
Ni(S_2)	+0.266	−0.133	0.94, 0.53	
Pd(S_2)	+0.54	−0.27	0.48, 0.76	
Pt(S_2)	+0.50	−0.25	0.56, 0.72	

[a] Calculations used B3LYP/6-311+G(3df)/SDD. [b] Orbital occupancy given first. Smaller corresponding antibonding π occupancies of 0.16, 0.20, 0.19, 0.24, 0.27, 0.27, respectively. The NBO calculation failed to find a bond between the metal and disulfur in the M(S_2) complexes.

TABLE 4: Calculated Structural Parameters and Vibrational Frequencies (cm^{-1}) for Group 10 Bisdioxygen Complexes[a]

complex	state	lengths, Å; angles, deg	frequencies, cm^{-1} (symmetry, intensities, km/mol)
$Ni(O_2)_2$	$^3B_{1u}$	NiO: 1.842; OO: 1.305; ONiO: 138.5°	1239.8 (a_g, 0), 1193.4 (b_{1u},271), 572.2 (b_{1u},1), 571.7 (b_{2u},0), 430.1(b_{3g},0), 426.2 (a_g,0), 267.1 (a_u,0), 189.0 (b_{3u},5), 158.8 (b_{2u},1)
$Pd(O_2)_2$	$^3B_{1u}$	PdO: 2.056; OO: 1.283; OPdO: 143.6°	1296.3 (a_g, 0), 1236.3 (b_{1u},436), 515.9 (b_{2u},1), 481.4 (b_{1u},37), 377.5 (a_g,0), 319.8 (b_{3g},0), 269.1 (a_u,0), 141.0 (b_{3u},0), 123.4 (b_{2u},0)
$Pd(O_2)_2$	$^3B_{1u}$	PtO: 2.040; OO: 1.301; OPtO: 142.8°	1247.0 (a_g, 0), 1196.8 (b_{1u},274), 460.4 (b_{1u},20), 441.4 (a_g,0), 431.2 (b_{2u},0), 424.1 (b_{3g},0), 285.6 (a_u,0), 159.2 (b_{3u},0), 142.1 (b_{2u},0)

[a] B3LYP/6-311+G(3df)/SDD.

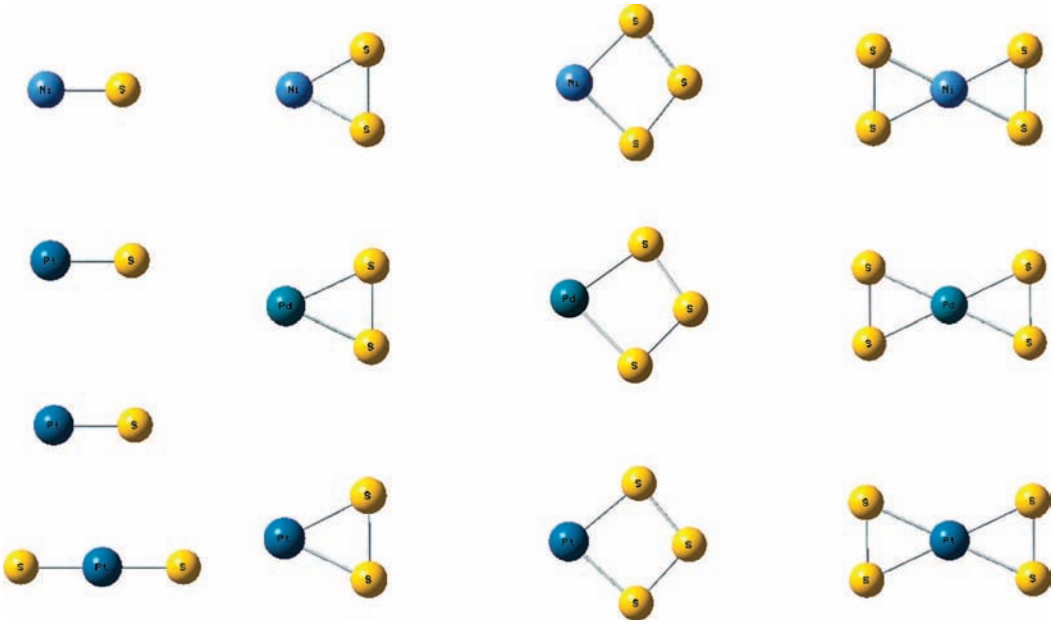

Figure 6. Structures calculated (B3LYP/6-311+G(3df)/SDD) for group 10 metal sulfur species.

SPtS. The 512.2 cm^{-1} band shifts to 500.6 cm^{-1} on sulfur-34 substitution, and the 1.0232 isotopic frequency ratio reveals significant Pt participation in this vibrational mode. These bands become an asymmetric 1/2/1 mixed isotopic triplet with mixed sulfur 32, 34 where the intermediate component is due to the single mixed isotopic product with two equivalent S atoms. Accordingly, the SPtS molecule was calculated and found to be linear with a strong antisymmetric stretching mode at 525.9 cm^{-1} and symmetry forbidden symmetric stretching mode at 508.7 cm^{-1}. The mixed isotopic component is 1.7 cm^{-1} higher than the median of pure isotopic positions due to interaction with the symmetric mode counterpart, which are of the same symmetry in the mixed isotopic molecule. Our DFT calculation finds this mode 23 cm^{-1} lower with 10% of the intensity of the antisymmetric counterpart observed here at 508.1 cm^{-1}. The weak 484.4 cm^{-1} band is tentatively assigned to this symmetric mode of the $^{32}SPt^{34}S$ isotopic molecule. Furthermore, our calculation predicts the antisymmetric stretching mode for $^{32}SPt^{34}S$ 2.1 cm^{-1} higher than the median calculated position, which substantiates agreement between calculated and observed frequencies and sulfur isotopic shifts for the new SPtS platinum disulfide molecule. The observation of SPtS on deposition with laser-ablated Pt atoms with S_2 molecules, with no growth on annealing, suggests that activation energy is required for the insertion reactions. Similar observations have been made for the OPtO molecule in solid argon and neon.[11,12] When searching for the infrared spectrum of the PtS molecule in the gas phase, look for the much more intense absorption of SPtS, which we predict near 515 cm^{-1}.

Pt(S$_2$). The weak 534.2 cm^{-1} band that increases on annealing shifts to 518.4 cm^{-1} with sulfur-34, and this high 32/34 isotopic frequency ratio (1.0305) is in accord with the pure S−S stretching mode of a S_x subunit. A possible product is $Pt(S_3)$, but our DFT calculation for the ground state produces a strong mode at 478 cm^{-1}, which is clearly too low for such an assignment. However, the side-bound $Pt(S_2)$ complex is only 8 kcal/mol higher than the SPtS minimum energy species, and its highest calculated frequency is 535 cm^{-1}. The potential energy surface is very flat on the question of equivalence of the two side-bound sulfur atoms. We likely observe two weak intermediate components, which suggests that the two sulfur atoms are not equivalent, but these bands are weak and their identification is tentative. The weak 534.2 cm^{-1} band that increases on annealing can be assigned with confidence to $Pt(S_2)$, which is formed without activation energy. Recall that both $Pt(O_2)$ and OPtO were observed in the dioxygen reaction, and in this case the side-bound complex is 41 kcal/mol higher in energy.[11,12] On the basis of the observation of $Pt(O_2)$ with thermal Pt atoms and OPtO with laser-ablated Pt atoms and on photolysis of $Pt(O_2)$,[9,11,12] it is clear that $Pt(O_2)$ is formed without activation energy and the inserted dioxide OPtO requires activation energy.

PtS. The weak 491.7 cm^{-1} band sharpens on annealing and shifts 12.4 cm^{-1} to 479.3 cm^{-1} on sulfur-34 substitution, and no mixed isotopic components are observed. The best prediction of the PtS vibrational fundamental comes from Dunham coefficients derived from the microwave spectrum,[20] but this 507 cm^{-1} value may be in error by up to 10 cm^{-1}. Our DFT calculation predicts 500.5 cm^{-1}, which is an oversimplification for this Hund's case (c) molecule. Nevertheless, the mechanics are accurate, and a 12.8 cm^{-1} sulfur-34 shift is predicted in the harmonic approximation, which is in excellent agreement with our observed 12.4 cm^{-1} sulfur-34 shift. A major part of this discrepancy is due to anharmonicity in the Pt−S vibration.

It is noteworthy that the PtO fundamental is below the antisymmetric stretching mode for the OPtO molecule, which has been observed in both solid argon and neon.[11,12] In fact, the gas-phase PtO fundamental is 1.4 cm^{-1} above the neon matrix PtO, a value that is 11.7 cm^{-1} higher than the 828.0 cm^{-1} argon matrix band. Extending these PtO data to PtS predicts the gas-phase PtS fundamental to be 1.6% or 7.8 cm^{-1} higher than the argon matrix band observed here, which is then 499.5 cm^{-1}. Hence, we suggest that the microwave and matrix infrared observations are pointing to a PtS vibrational fundamental very near 500 cm^{-1} in the gas phase.

Reaction Mechanisms. The argon discharge produces $S_{1,2,3,4}$ for codeposition with laser-ablated group 10 metal atoms, so a variety of reactions are possible in these experiments. The NiS and PtS molecules can be produced in the direct atom combination reaction or in the abstraction reaction from S_2 or S_3, which are computed to be 28 or 19 kcal/mol exothermic for NiS. The combination reaction (3) is calculated to be 46 kcal/mol exothermic for Pd, which is observed here and is reminiscent of the alkali metal ozonides formed by direct reactions.[40]

$$M + S \rightarrow MS \tag{1}$$

$$Ni + S_2 \rightarrow NiS + S \tag{2a}$$

$$Ni + S_3 \rightarrow NiS + S_2 \tag{2b}$$

$$Pd + S_3 \rightarrow PdS_3 \tag{3}$$

The $M(S_2)_2$ molecules are observed to be dominant product absorptions for all three metals, but the $M(S_2)$ molecules are stable with very weak absorptions. Interestingly, if the infrared intensities (Table 2) are taken into account, the $Ni(S_2)$ and $Pt(S_2)$ absorptions after 40 K annealing in Figures 1 and 4 represent more molecules than the stronger $Ni(S_2)_2$ and $Pt(S_2)_2$ absorptions. In the case of the $M(O_2)_2$ molecules, it was believed that $M(O_2)$ is formed first and then a second O_2 molecule is added,[8−12] and that mechanism given in spontaneous reactions (4) and (5) surely contributes to the present reactions. There is another mechanism possible with sulfur due to the known presence of the S_4 molecule in the reagent mix,[23] and that is direct reaction (6). In the cases of Ni and Pd, the side-bound complexes are the minium energy species, but the global minimum energy structure for Pt is SPtS, which is clearly observed here. We anticipate that cyclic $Pt(S_2)$ is formed without activation energy, but that the insertion reaction (7) requires excited Pt produced in the laser ablation process.

$$M + S_2 \rightarrow M(S_2) \tag{4}$$

$$M(S_2) + S_2 \rightarrow M(S_2)_2 \tag{5}$$

$$M + S_4 \rightarrow M(S_2)_2 \tag{6}$$

$$Pt + S_2 \rightarrow SPtS \tag{7}$$

Bonding. Several interesting comparisons can be made for bonding in the bisdioxygen and bisdisulfur complexes. The computed Mulliken charges[35] show a small amount of charge transfer from metal to ligand except for $Ni(S_2)_2$ where the Mulliken spin densities also indicate more electron spin remains on the metal center in the Ni than in the Pt case (Table 3). Despite the fact that both nickel (d^8s^2, ^3F) and platinum (d^9s^1, ^3D) atoms are triplet states,[41] the spin densities in these metal complexes are distributed to the ligand atomic centers in the ligand bonding and back-bonding interaction. Recall that Pd is a singlet state (d^{10}, ^1S) and that the S_2 reagent is a triplet state ($^3\Sigma_g^-$). Interestingly, the Ni and Pt centers retain more spin density in the disulfur than in the dioxygen complexes. The complex bonding interaction for each ligand is bonding π to metal sd hybrid, and this bonding orbital contains a higher proportion of oxygen contribution than sulfur. Furthermore, the antibonding orbital occupancy is greater for the sulfur than for the oxygen products. The simple $M(S_2)$ complexes exhibit a reduction of spin density for all atoms save Pd in the bonding and back-bonding interactions. The appearance of spin density on Pd requires charge transfer to the S_2 ligand, which is corroborated by the Mulliken charges. Our calculated S−S bond length in $Ni(S_2)$ of 2.070 Å is near that measured for NiS_2 in the pyrite structure (2.065 Å), although our Ni−S distance of 2.155 Å in this molecule is much shorter than that found in the solid compound (2.396 Å).[42]

Conclusions

Laser-ablated Ni, Pd, and Pt atoms reacted with sulfur molecules emerging from a microwave discharge in argon during condensation at 7 K. New absorptions in the matrix infrared spectra were assigned on the basis of sulfur isotopic shifts, spectra of sulfur isotopic mixtures, and frequencies from density functional calculations. The strongest absorptions were observed at 597.9, 596.1, and 583.6 cm^{-1}, respectively, for the group 10 metals. These absorptions exhibited large sulfur-34 shifts and 32/34 isotopic frequency ratios (1.0282, 1.0285, 1.0298) that are appropriate for S−S stretching modes. Diagnostic 1/4/4/2/4/1 sextet mixed 32/34 isotopic multiplets identify this product with two equivalent S_2 molecules containing equivalent atomic positions as the bisdisulfur complexes $M(S_2)_2$. Our DFT calculations find stable D_{2h} structures with B_{1u} ground states and intense b_{1u} infrared active S−S stretching modes a few wavenumbers higher than was observed. In contrast, the simple $M(S_2)$ complexes have very weak a_1 S−S stretching modes, which are observed in accord with calculations for the $^3B_1$ ground states. Harmonic frequencies calculated with the B3LYP density functional are usually slightly higher than the observed values,[43] and it is gratifying that these calculations work so well for transition metal sulfur species, which could easily have been difficult subjects for electronic structure calculations.

A minor product with Ni at 505.8, 502.7 cm^{-1} shows the proper sulfur-34 shift and 32/34 isotopic frequency ratios (1.01914, 1.01926) for assignment to ^{58}NiS, ^{60}NiS. Another major product with Pt at 512.2 cm^{-1} reveals an asymmetric triplet absorption with mixed sulfur 32/34 and isotopic frequency ratio 1.0232, which is appropriate for assignment to the SPtS disulfide molecule. This molecule is predicted by DFT to be linear with strong σ_u mode at 526 cm^{-1}. A weak 491.7 cm^{-1} peak exhibits the sulfur-34 shift and isotopic frequency ratio (1.0259) expected for PtS, and this assignment leads to a 500 cm^{-1} prediction for the gas-phase frequency.

Acknowledgment. We gratefully acknowledge financial support from the National Science Foundation, and helpful correspondence with P. Bernath and permission to quote unpublished results.

References and Notes

(1) (a) *Transition Metal Sulfur Chemistry, Biological and Industrial Significance*; Stiefel, E. I., Matsumoto, K., Eds.; American Chemical Society: Washington, DC, 1997. (b) *Transition Metal Sulphides, Chemistry and Catalysis*; Weber, T., Prins, R., van Santen, R. A., Eds.; NATO ASI Series; Kluwer Academic Publishers: The Netherlands, 1998.

(2) Wang, J. H.; Cheng, Z.; Bredas, J. L.; Liu, M. L. *J. Chem. Phys.* **2007**, *127*, 214705.

(3) Dong, J.; Cheng, Z.; Zha, S.; Liu, M. L. *J. Power Sources* **2006**, *156*, 461.

(4) Xie, B.; Jiang, Y.; Yuan, S. W. *Chem. Lett.* **2002**, 254.

(5) Oviedo-Roa, R.; Martinez-Magadan, J. M.; Illas, F. *B* **2006**, *110*, 7951.

(6) O'Mahoney, A. M.; Silvester, D. S.; Aldous, L.; Hardacre, C.; Compton, R. G. *J. Phys. Chem. C* **2008**, *112*, 7725.

(7) Malik, M. A.; O'Brien, P.; Revaprasadu, N. *J. Mater. Chem.* **2002**, *12*, 92.

(8) Huber, H.; Ozin, G. A. *Can. J. Chem.* **1972**, *50*, 3746.

(9) Huber, H.; Klotzbucher, W.; Ozin, G. A.; Vander Voet, A. *Can. J. Chem.* **1973**, *51*, 2722.

(10) Citra, A.; Chertihin, G. V.; Andrews, L.; Neurock, M. *J. Phys. Chem. A* **1997**, *101*, 3109; (Ni + O_2).

(11) Bare, W. D.; Citra, A.; Chertihin, G. V.; Andrews, L. *J. Phys. Chem. A* **1999**, *103*, 5456; Pd, Pt + O_2 in argon.

(12) Wang, X.; Andrews, L. *J. Phys. Chem. A* **2001**, *105*, 5812; Pd, Pt + O_2 in neon.

(13) Liang, B.; Andrews, L. *J. Phys. Chem. A* **2002**, *106*, 3738; V, Nb, Ta + S_2.

(14) Liang, B.; Andrews, L. *J. Phys. Chem. A* **2002**, *106*, 6295; Ti, Zr, Hf + S_2.

(15) Liang, B.; Andrews, L. *J. Phys. Chem. A* **2002**, *106*, 4038; Th + S_2.

(16) Liang, B.; Andrews, L.; Ismail, N.; Marsden, C. J. *Inorg. Chem.* **2002**, *41*, 2811; U + S_2.

(17) DeVore, T. C.; Franzen, H. F. *High Temp. Sci.* **1975**, *7*, 220. The 536 cm^{-1} Ni and OCS reaction product first assigned to NiS is due to some other species.

(18) Yamamoto, T.; Tanimoto, M.; Okabayashi, T. *Phys. Chem. Chem. Phys.* **2007**, 3744.

(19) Li, B. Z.; Jung, K. Y.; Steimle, T. C. *J. Mol. Spectrosc.* **1995**, *170*, 310.

(20) Cooke, S. A.; Gerry, M. C. L. *J. Chem. Phys.* **2004**, *121*, 3486.

(21) Bauschlicher, C. W., Jr.; Maitre, P. *Theor. Chim. Acta* **1995**, *90*, 189.

(22) Bridgeman, A. J.; Rothery, J. *J. Chem. Soc., Dalton Trans.* **2000**, 211.

(23) Brabson, G. D.; Mielke, Z.; Andrews, L. *J. Phys. Chem.* **1991**, *95*, 79 (sulfur vapor discharge, infrared spectra).

(24) Thorwirth, S.; McCarthy, M. C.; Gottlieb, C. A.; Thaddeus, P.; Gupta, H.; Stanton, J. F. *J. Chem. Phys.* **2005**, *123*, 054326, and references therein.

(25) Peterson, K. A.; Lyons, J. R.; Francisco, J. S. *J. Chem. Phys.* **2006**, *125*, 084314.

(26) Matus, M. H.; Dixon, D. A.; Peterson, K. A.; Harkless, J. A. W.; Francisco, J. S. *J. Chem. Phys.* **2007**, *127*, 174305.

(27) (a) Long, S. R.; Pimentel, G. C. *J. Chem. Phys.* **1977**, *66*, 2219. (b) Smardzewski, R. R. *J. Chem. Phys.* **1978**, *68*, 2878.

(28) Andrews, L.; Citra, A. *Chem. Rev.* **2002**, *102*, 885, and references therein.

(29) Andrews, L.; Cho, H.-G. *Organometallics* **2006**, *25*, 4040, and references therein (review article).

(30) Cho, H.-G.; Andrews, L. *J. Am. Chem. Soc.* **2008**, *130*, 15836.

(31) Frisch, M. J.; *Gaussian 98*, revision A.1; Gaussian, Inc.: Pittsburgh, PA, 1998.

(32) (a) Becke, A. D. *J. Chem. Phys.* **1993**, *98*, 5648. (b) Lee, C.; Yang, Y.; Parr, R. G. *Phys. Rev. B* **1988**, *37*, 785.

(33) Raghavachari, K.; Trucks, G. W. *J. Chem. Phys.* **1989**, *91*, 1062.

(34) Hay, P. J.; Wadt, W. R. *J. Chem. Phys.* **1985**, *82*, 270. Wadt, W. R.; Hay, P. J. *J. Chem. Phys.* **1985**, *82*, 284. Hay, P. J.; Wadt, W. R. *J. Chem. Phys.* **1985**, *82*, 299.

(35) Frisch, M. J.; *Gaussian 03*, revision B.04; Gaussian, Inc.: Pittsburgh, PA, 2003.

(36) Andrae, D.; Haeussermann, U.; Dolg, M.; Stoll, H.; Preuss, H. *Theor. Chim. Acta* **1990**, *77*, 123.

(37) (a) Reed, A. E.; Weinstock, R. B.; Weinhold, F. *J. Chem. Phys.* **1985**, *83*, 735. (b) Reed, A. E.; Curtiss, L. A.; Weinhold, F. *Chem. Rev.* **1988**, *88*, 899.

(38) The natural abundances of ^{58}Ni and ^{60}Ni are 68.3% and 26.1%. *CRC Handbook of Chemistry and Physics*; CRC Press: Boca Raton, FL, 1985.

(39) Bernath, P. Personal communication of unpublished results, Nov. 2008.

(40) Spiker, R. C., Jr.; Andrews, L. *J. Chem. Phys.* **1973**, *59*, 1851.

(41) Moore, C. E. Atomic Energy Levels, N. B. S. Circ. 467, 1958.

(42) Wells, A. F. *Structural Inorganic Chemistry*, 4th ed.; Clarendon: Oxford, 1975.

(43) (a) Scott, A. P.; Radom, L. *J. Phys. Chem.* **1996**, *100*, 16502. (b) Andersson, M. P.; Uvdal, P. L. *J. Phys. Chem. A* **2005**, *109*, 3937.

JP810795Q